

Article

The Synergistic Effect of Simultaneous Ultrasound Heating and Disintegration on the Technological Efficiency and Energetic Balance of Anaerobic Digestion of High-Load Slaughter Poultry Sewage

Joanna Kazimierowicz ^{1,*} , Marcin Dębowski ²  and Marcin Zieliński ² 

¹ Department of Water Supply and Sewage Systems, Faculty of Civil Engineering and Environmental Sciences, Białystok University of Technology, 15-351 Białystok, Poland

² Department of Environment Engineering, Faculty of Geoengineering, University of Warmia and Mazury in Olsztyn, 10-720 Olsztyn, Poland

* Correspondence: j.kazimierowicz@pb.edu.pl

Abstract: Regulations in force urge for thermal pre-treatment of post-slaughter waste prior to its anaerobic digestion. Increased interest in biomethane as a fuel in gas networks or vehicles of road transport forces the need to look for heating methods that are alternative to heat recovery from cogeneration. The goal of this study was to determine the synergistic effect of simultaneous ultrasound heating and disintegration on the technological efficiency and energetic balance of the anaerobic digestion of high-load slaughter poultry wastewater. The highest efficiency of anaerobic digestion was obtained for the ultrasound thermal pre-treatment (60 min, 90 °C, OLR = 2.0 gCOD/dm³). In this experimental variant, the biogas production rate reached 9.0 ± 0.2 cm³/gCOD·h, biogas yield was 492 ± 10 cm³/gCOD, and the biogas produced contained 69.8 ± 1.4% CH₄. Given the incurred energy outputs, the highest net energetic efficiencies, i.e., 5.92 ± 0.43 Wh and 5.80 ± 0.42 Wh, were obtained in the variants with the conventional thermal pre-treatment (60 min, 70 °C, OLR = 6.0 gCOD/dm³) and ultrasound thermal pre-treatment (60 min, 70 °C, OLR = 6.0 gCOD/dm³), respectively.

Keywords: post-slaughter wastewater; high-load wastewater; thermal pre-treatment; ultrasounds; disintegration; anaerobic digestion; biogas



Citation: Kazimierowicz, J.; Dębowski, M.; Zieliński, M. The Synergistic Effect of Simultaneous Ultrasound Heating and Disintegration on the Technological Efficiency and Energetic Balance of Anaerobic Digestion of High-Load Slaughter Poultry Sewage. *Appl. Sci.* **2023**, *13*, 2420. <https://doi.org/10.3390/app13042420>

Academic Editor: José Carlos Magalhães Pires

Received: 29 January 2023

Revised: 9 February 2023

Accepted: 12 February 2023

Published: 13 February 2023



Copyright: © 2023 by the authors. Licensee MDPI, Basel, Switzerland. This article is an open access article distributed under the terms and conditions of the Creative Commons Attribution (CC BY) license (<https://creativecommons.org/licenses/by/4.0/>).

1. Introduction

In the last decade, poultry meat consumption in the European Union increased from 20.6 kg per capita/year in 2010 to 23.5 kg per capita/year per person in 2021 [1,2]. This increase is chiefly reflected in a growing number of producers as well as the increased amount of raw material processed and loads of post-slaughter waste and highly polluted sewage generated [3]. Due to the potential adverse impact on the natural environment, susceptibility to putrefaction, and sanitary risk, their handling is strictly regulated by law [4]. They can be a substrate featuring a vast potential for use in utilization biogas plants. This type of biomass is characterized by a high content of organic compounds susceptible to biodegradation, which directly affects the increase in the volume and improvement in the quality of the biogas produced [5].

Wastes generated in the meat processing plants are by-products posing a low sanitary risk. They are included in three categories of wastes, i.e., animal-derived by-products recognized as suitable for consumption, foodstuffs of animal origin that pose no threat to animal and human health, and withdrawn foodstuffs of animal origin [6]. The rules for dealing with this type of waste are stipulated in the provisions of Regulation (EC) No. 1069/2009 of the European Parliament and of the Council of 21 October 2009 as they laid down sanitary rules for animal by-products not intended for human consumption [7]. One of the acceptable and promoted means of neutralizing this type of waste is its transformation

into biogas, fertilizers, and soil improvers [8]. The requirements for its hygienization before the anaerobic digestion process are to keep the material pre-disintegrated to a maximum particle diameter of 60 mm at 70 °C for 60 minutes, according to the provisions of the Regulation of the European Commission No. 142/2011 of 25 February 2011 on the implementation of Regulation (EC) No. 1069/2009 of the European Parliament and of the Council [9].

The thermal pre-treatment of post-slaughter waste is carried out mainly via hydrothermal depolymerization or thermochemical methods [10]. It allows for the effective hygienization of the processed medium as well as the destruction and release of complex organic molecules into the dissolved phase [11]. Hydrolysates are used in an easier and more accessible way by extracellular enzymes of anaerobic microorganisms, which leads to an improvement in anaerobic degradation efficiency [12]. Multiple methods of heat treatment of post-slaughter waste have been developed and tested so far. They differ in the source and method of heat supply, the range of temperatures used, the retention time during hydrothermal depolymerization, and the methods of chemical catalysis [13].

Waste heat from cogeneration systems was often used for the legally required thermal treatment of category 3 (C3) waste prior to the process of anaerobic digestion [14]. This method of biogas management allows for the production of electricity and significant amounts of low-temperature waste heat that is difficult to manage but can be used to heat post-slaughter waste (60 min, 70 °C). Currently, other competitive ways of exploiting biogas are increasingly deployed. In many cases, it is more reasonable from the economic and environmental points of view to enrich and refine raw biogas into biomethane, and then to inject it into gas networks or use it directly to power engines of agricultural machines or public transport vehicles [15]. Such alternative avenues of biogas exploitation eliminate waste heat generation in the biogas plant facility, which can be used for the thermal pre-treatment of C3 waste [16]. Therefore, there is a justified need to look for other competitive methods of heating organic substrates which can boost the final effects of methane fermentation.

So far, little attention has been paid to the possibility of using ultrasounds (UD) in the combined process of ultrasonic disintegration and hydrothermal depolymerization. One of the mechanisms of UD action, being of great biological and technological importance, is its thermal effect [17]. It is the result of the absorption of acoustic energy by matter and its conversion into heat. The thermal effect achieved is affected by the initial temperature of the medium, the level of dynamic balance between heat collection and heat release, heat losses, absorption capacity, ultrasonic energy dissipation processes, the presence of insulators, and the UD characteristics, including intensity and frequency [18]. The final increase in the temperature of the medium to which the UD is emitted and the extent of disintegration of the matter present in this medium are also affected by the non-thermal phenomena, the most important of which include cavitation and stresses [19].

In the systems exposed to UD, stresses appear, which can cause numerous changes in the structure of molecules. They are either the effect of ultrasonic pressure, the forces related to the change in viscosity, or biological object movement in the medium [20]. UD propagating in the fluid may cause twisting, rotation, or spinning of suspended elements, mainly macromolecules with asymmetric shapes [21]. The stresses associated with the jet flow can trigger changes in the charge of the cell surface and permeability of the cell membrane, and also cause the rupture, disintegration, and fragmentation of the cell membrane [22]. The phenomenon of cavitation consists in the formation of pulsating vacuum bubbles in the liquid, sometimes filled with saturated steam or gas dissolved in the liquid [23]. Cavitation bubbles appear as a result of local bursting of the medium under the influence of large tensile forces. Then, they can expand and pulsate in a forced way with UD waves or collapse in the phase of wave densification, producing sudden pressure changes and local shock waves [24]. It has been observed that the cavitation bubbles are deformed into funnel-shaped vortices directed at the liquid/solid interface with their tip, accelerating the processes of disintegration, degradation, and erosion of

solids [25]. Particles suspended in the liquid in the vicinity of pulsating and oscillating cavitation bubbles can be drawn into the region of a high velocity gradient. Then, the bubble oscillating around the cell membrane causes its vibrations and leads to stream movements in the biomass structure [26]. As a result of these processes, the cell is exposed to shear stresses, which may cause its damage and disintegration [27].

The inspiration for planning and carrying out the research in question was to verify whether the use of ultrasound waves for thermal treatment of category 3 (C3) waste, required by law, will result in a synergistic technological effect associated with simultaneous thermal pre-treatment and ultrasonic disintegration. The aim was to determine whether the applied technological solution would have a direct impact on the volume of biogas produced and the methane content. Based on data obtained, the energy balance and energy efficiency of the tested solution were also determined and compared to these of conventional heating. The main objective of this research was to determine the effect of applying UD in the thermal pre-treatment of H-LSPW on the efficiency and energy balance of the anaerobic digestion process compared to conventional heating.

2. Materials and Methods

2.1. Concept of Research Works

The study was divided into 4 stages (S) differing in the methods of pre-treatment of high-load slaughter poultry wastewater (H-LSPW) prior to anaerobic digestion (AD). Initially homogenized H-LSPW was either not subjected to thermal pre-treatment (E0) or subjected to conventional thermal pre-treatment (CTP) under conditions as follows: S1—60 min CTP (70 °C), S2—60 min CTP (90 °C); or, subjected to ultrasound thermal pre-treatment (UTP) under conditions as follows: S3—60 min UTP (70 °C) and S4—60 min UTP (90 °C). Each of the stages was divided into 3 variants (V) differing in the initial organic load rate (OLR) of the anaerobic respirometers: V1—2.0 gCOD/dm³, V2—4.0 gCOD/dm³, and V3—6.0 gCOD/dm³. The AD process was conducted at a temperature of 42 °C.

2.2. Materials

The study tested the H-LSPW from a meat processing plant, after the slaughter of turkeys, and then after the production of packaged meat, including schnitzels, turkey breast fillets, thighs and drumsticks, tenderloins, knuckles, livers, necks, gizzards, wings, and hearts. The processing plant offers a wide range of sausages and a wide range of cold cuts, including cooked fillets and breasts, hams, tenderloins, mortadella, and a wide range of pâtés. The production generates on average 1200 m³/d H-LSPW, including nearly 16 m³ of blood and 25 tons/d of soft post-slaughter wastes, including crops, esophagi, tracheas, lungs, bladders, intestines, and undigested food from crops, gizzards, and intestines. Table 1 presents the characteristic contaminants of the H-LSPW tested during the experiment.

Table 1. Characteristics of H-LSPW used in AD.

Indicator	Unit	Value
Total solids (TS)	[%]	1.03 ± 0.13
Mineral solids (MS)	[%TS]	12.1 ± 0.41
Volatile solids (VS)	[%TS]	87.9 ± 0.41
Total nitrogen (TN)	[mgN/dm ³]	6800 ± 1290
Ammonium (N-NH ₄ ⁺)	[mgN-NH ₄ /dm ³]	4120 ± 1640
Total phosphorus (TP)	[mgP/dm ³]	480 ± 202
Orthophosphate (P-PO ₄ ³⁻)	mg P-PO ₄ /dm ³	291 ± 61
Protein	[mg/dm ³]	42,500 ± 8810
Lipids	[mg/dm ³]	31,700 ± 5190
Carbohydrates	[mg/dm ³]	2670 ± 970
Chemical oxygen demand (COD)	[mgO ₂ /dm ³]	72,930 ± 4950

Table 1. *Cont.*

Indicator	Unit	Value
Biological oxygen demand (BOD ₅)	[mgO ₂ /dm ³]	59,260 ± 3030
Total organic carbon (TOC)	[mg/dm ³]	28,640 ± 1470
COD:N ratio	-	10.72 ± 1.52
BOD ₅ :N ratio	-	8.71 ± 1.13
TOC:N ratio	-	4.22 ± 0.76
pH	-	6.78 ± 0.05

The anaerobic sludge was sourced from an agricultural biogas plant and operated on at a technical scale, in which a mixture of substrates based on waste from turkey houses, maize silage, and post-slaughter waste was fermented. The technological operational parameters of the plant were as follows: OLR = 2.8 kgVS/m³·d, HTR = 42 days, fermentation temperature T = 42 ± 1 °C. Prior to AD, the post-slaughter waste (category K3) was disintegrated to an average particle size of 40 mm and thermally pre-treated at 70 °C for 60 minutes. Table 2 presents the characteristics of anaerobic sludge inoculum used in the experiment.

Table 2. Characteristics of anaerobic sludge biomass.

Indicator	Unit	Value
TS	[%]	5.7 ± 1.1
VS	[% TS]	76.9 ± 2.0
MS	[% TS]	23.1 ± 1.9
TN	[mg/gTS]	71.3 ± 9.6
TP	[mg/gTS]	11.7 ± 1.3
TC	[mg/gTS]	882 ± 104.7
TOC	[mg/gTS]	690.8 ± 58.3
C:N ratio	-	12.4 ± 0.9
pH	-	7.07 ± 0.12
Protein	[% DM]	44.6 ± 3.3
Lipids	[% DM]	14.1 ± 1.5
Saccharides	[% DM]	3.7 ± 0.9

2.3. Laboratory Equipment

The process of initial fragmentation and homogenization of the H-LSPW was carried out using a laboratory knife mill PULVERISETTE 11 (Fritsch GmbH, Idar-Oberstein, Germany). The H-LSPW feedstock to the mill was 1.0 dm³. The fragmentation process was carried out using a four-bladed titanium knife operating at a rotational speed of 10,000 rpm for 90 seconds. The CTP and UTP were carried out in the IS-1K reactor (InterSonic, Olsztyn, Poland), in which the H-LSPW was heated using electric heaters or ultrasonic waves, depending on the experimental stage. Then, 1.0 dm³ of pre-homogenized and disintegrated H-LSPW was introduced into the IS-1K reactor chamber. In S1 and S2, the substrate was heated using a set of electrical heaters with a power of 500 W, whereas in S3 and S4, the substrate was treated with ultrasounds having the frequency of 35 kHz and power of 400 W. The IS-1K reactor was thermally insulated with 10 cm³ thick polystyrene to prevent heat loss. In all experimental stages, energy consumption for heating was monitored by means of an Orno OR-WAT-435 watt meter (Elmak Ltd., Rzeszów, Poland). In S1 and S3, the H-LSPW temperature was kept within the range of 70 °C to 73 °C, whereas in S2 and S4 it was kept within the range of 90 °C to 93 °C. Electrical heaters or ultrasound heads were started and stopped automatically when the temperature limits had been reached. The control system was integrated with a Pt100 temperature sensor (Jumo Ltd., Wrocław, Poland) monitoring the temperature in the H-LSPW.

The AD analyses were conducted with the use of kits for the OxiTop[®]-IDS AN 6 Anaerobic Degradation Measuring System (WTW, Cologne, Germany). The system registers biogas partial pressure changes in a measuring chamber. In each experimental variant,

500 cm³ of anaerobic sludge were fed to digesters followed by the assumed doses of H-LSPW (V1—1.0 gCOD ≈ 14 cm³, V2—2.0 gCOD ≈ 24 cm³, and V3—3.0 gCOD ≈ 48 cm³). Measurements were performed at a temperature of 42 ± 1 °C. AD was continued for 20 days, with pressure changes registered in the digester every 6 h. To ensure anaerobic conditions, the digester was purged with nitrogen for 5 min with the efficiency of 100 dm³/min.

2.4. Analytical Methods

The contents of COD, TP, P-PO₄, TN, and N-NH₄ were determined using a DR 5000 spectrophotometer with an HT 200 s mineralizer (Hach-Lange GmbH, Düsseldorf, Germany). The BOD₅ was determined according to Polish Standard PN-EN 1899-1. The TOC content was determined by means of a TOC-L analyzer (Shimadzu, Kyoto, Japan). In turn, the contents of TS, VS, and MS were determined with the gravimetric method (PN-EN 15935:2022-01). The contents of TC, TOC, and TN were assayed using a Flash 2000 analyzer (Thermo Scientific, Waltham, MA, USA), whereas the TP content was determined colorimetrically at the wavelength of 390 nm (DR 2800 spectrophotometer, Hach-Lange GmbH, Düsseldorf, Germany) after earlier mineralization. The total protein content was estimated by multiplying the TN concentration by a multiplication of 6.25. The sugars were analyzed at the wavelength of 600 nm, using a DR 2800 spectrophotometer (Hach-Lange GmbH, Dusseldorf, Germany). Lipids were extracted using the Soxhlet method with a Buchi extraction apparatus (Flawil, Switzerland), and then their content was determined by weight difference. The pH value was measured using an HQ11D pH-meter (Hach-Lange GmbH, Düsseldorf, Germany). In turn, the contents of COD, TOC, and BOD₅ in the dissolved phase were determined after H-LSPW filtration using a kit for membrane vacuum filtration (Advantec MFS, Inc., Dublin, CA, USA) [17]. The composition of biogas produced was determined every 24 h using a gas chromatograph (GC, 7890A Agilent, Santa Clara, CA, USA).

2.5. Computation Methods

The real energy input (E_{wpT}) was sourced from measurements made with the Orno OR-WAT-435-watt meter (Elmco Ltd., Poland). The energy output (E_{CH_4out}) generated from methane production was calculated using the following equation:

$$E_{CH_4out} = Y_{CH_4out} \times E_{CH_4} \times M_{CODin} \text{ [Wh]} \quad (1)$$

where:

Y_{CH_4out} —methane yield [dm³/g COD];

E_{CH_4} —methane energetic value (Wh/cm³); and

M_{CODin} —COD mass fed to the respirometer (gCOD).

The unit-specific energy input (E_{uin}) per COD_{in} mass load was calculated using Equation (2):

$$E_{uin} = E_{sin} / M_{CODin} \text{ [Wh/gCOD]} \quad (2)$$

where:

E_{uin} —unit specific energy input (Wh/g COD);

E_s —the specific energy input [Wh]; and

M_{CODin} —COD mass (g COD).

The total energy input to the respirometer (E_{totin}) was calculated using Equation (3):

$$E_{totinR} = E_{uin} / M_{CODinR} \text{ [Wh]} \quad (3)$$

where:

E_{totinR} —unit specific energy input to respirometer (Wh);

E_{uin} —unit specific energy input (Wh/g COD); and

M_{CODinR} —COD mass fed to the respirometer (g COD).

The net energy gain (E_{net}) was calculated according to Equation (4):

$$E_{\text{net}} = E_{\text{CH}_4\text{out}} - E_{\text{totinR}} \text{ [Wh]} \quad (4)$$

The respirometric measurements allowed for the determination of the rate of biogas production (r) and the reaction rate constant (k). An iterative method was deployed, in which the convergence coefficient (φ^2) between the model and the experimental data was assumed at 0.2. It represents the ratio of the sum of the squares of the deviations of the values calculated based on the determined function from the experimental values to the sum of the squares of the deviations of the experimental values from the mean value.

2.6. Statistical Analysis

To assess the significance of differences between variables, a one-way analysis of variance (ANOVA) and the Tukey (HSD) test were applied ($p = 0.05$) using the Statistica 13.1 PL package (Statsoft, Inc., Tulsa, OK, USA).

3. Results and Discussion

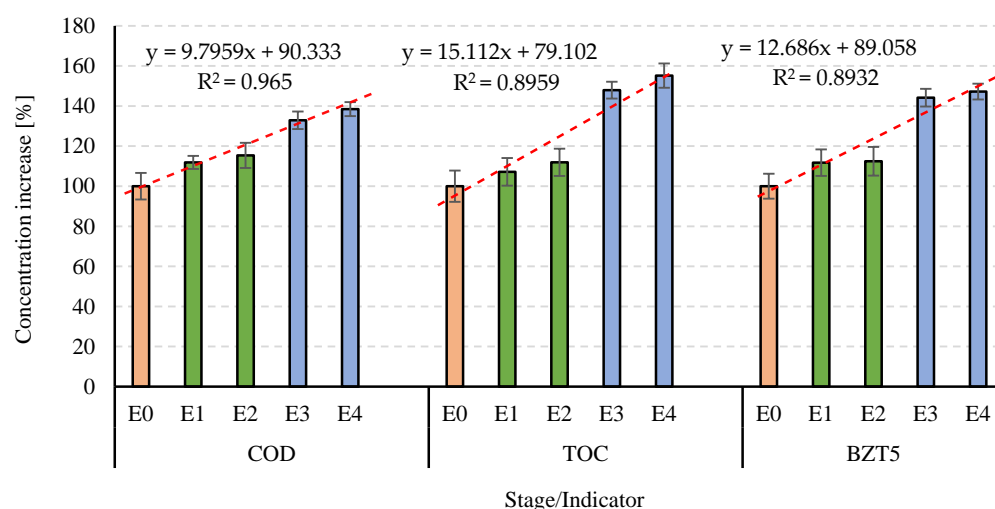
3.1. Concentrations of Organic Compounds in the Dissolved Phased

One of the ways to assess the efficiency of pre-treatment processes is to analyze the concentrations of selected indicators in the dissolved phase of the organic substrate undergoing disintegration [28]. Analyses conducted in this case usually entail monitoring concentrations of organic compounds and less frequently concentrations of sugars and suspended solids, as well as measurements of turbidity and color, and concentrations of nutrients or genetic material [29]. In some cases, it is possible to develop reliable correlations and models to estimate AD efficiency based on the presence of organic compounds in the dissolved phase [30,31]. For this reason, carrying out this type of assessment is useful from a practical point of view, as it reduces the need to conduct more advanced measurements in order to determine the efficiency of the applied pre-treatment methods [17].

In S0, where the H-LSPW was not subjected to thermal pre-treatment, the values of the analyzed indicators characterizing concentrations of organic compounds were as follows: $29,400 \pm 1950 \text{ mgO}_2/\text{dm}^3$ (COD), $11,580 \pm 1020 \text{ mg}/\text{dm}^3$ (TOC), and $21,370 \pm 1330 \text{ mgO}_2/\text{dm}^3$ (BOD₅) (Table 3). The use of CTP in S1 (70 °C) and S2 (90 °C) caused a significant increase in the concentrations of dissolved organic compounds to the values noted in S0. In contrast, no significant differences were found that would be dependent on CTP temperature (Figure 1). The COD values reached $32,890 \pm 1070 \text{ mgO}_2/\text{dm}^3$ in S1 and $33,920 \pm 2130 \text{ mgO}_2/\text{dm}^3$ in S2. In the respective experimental stages, the TOC values were $12,410 \pm 980 \text{ mg}/\text{dm}^3$ (an increase by $7.2 \pm 0.79\%$) and $12,960 \pm 1270 \text{ mg}/\text{dm}^3$ (an increase by $11.9 \pm 0.98\%$), whereas the BOD₅ values reached $23,880 \pm 1580 \text{ mgO}_2/\text{dm}^3$ (an increase by $11.7 \pm 0.66\%$) and $24,030 \pm 1720 \text{ mgO}_2/\text{dm}^3$ (an increase by $12.4 \pm 0.72\%$) (Table 3). The use of the combined process of thermal pre-treatment and ultrasound disintegration (UTP) allowed for a significant increase in the organic matter content in the dissolved phase (Figure 1). The highest COD, TOC, and BOD₅ values, reaching $40,710 \pm 1420 \text{ mgO}_2/\text{dm}^3$; $17,970 \pm 1090 \text{ mg}/\text{dm}^3$; and $31,460 \pm 1240 \text{ mgO}_2/\text{dm}^3$, respectively, were determined in S4. The achieved concentrations were due to the $38.5 \pm 0.35\%$ increase in COD, $55.2 \pm 0.61\%$ increase in TOC, and $47.2 \pm 0.39\%$ increase in BOD₅ (Table 3).

Table 3. Concentrations of organic compounds in the dissolved phase in individual experimental stages.

Stage		Indicator					
		COD		TOC		BOD ₅	
		Concentration [mgO ₂ /dm ³]	Increase [%]	Concentration [mg/dm ³]	Increase [%]	Concentration [mgO ₂ /dm ³]	Increase [%]
0	Raw wastewater	29,400 ± 1950	-	11,580 ± 1020	-	21,370 ± 1330	-
1	60 min, CTP (70 °C)	32,890 ± 1070	11.9 ± 0.35	12,410 ± 980	7.2 ± 0.79	23,880 ± 1580	11.7 ± 0.66
2	60 min, CTP (90 °C)	33,920 ± 2130	15.4 ± 0.63	12,960 ± 1270	11.9 ± 0.98	24,030 ± 1720	12.4 ± 0.72
3	60 min, UTP (70 °C)	39,070 ± 1710	32.9 ± 0.44	17,130 ± 720	47.9 ± 0.42	30,810 ± 1360	44.2 ± 0.44
4	60 min, UTP (90 °C)	40,710 ± 1420	38.5 ± 0.35	17,970 ± 1090	55.2 ± 0.61	31,460 ± 1240	47.2 ± 0.39

**Figure 1.** Effect of thermal pre-treatment method on the percentage increase in the concentration of organic compounds.

In the case of C3 waste, like the analyzed H-LSPW, the thermal pre-treatment is not an intended deliberate procedure but results from regulations in force advising the hygienization of this type of organic substrate [32]. Regardless of this fact, an expected technological outcome of the required thermal pre-treatment is the increased efficiency of methane fermentation. Undoubtedly, the disintegration of complex macromolecules of the biomass followed by the efficient transfer of organic compounds to the dissolved phase increases substrate availability to anaerobic bacteria [33]. The present study demonstrated a strong linear correlation between the thermal pre-treatment method and the efficiency of organic matter transfer to the dissolved phase. In the case of COD, the fit of the correlation reached $R^2 = 0.9650$, whereas in the case of TOC and BOD₅, the R^2 values were only slightly lower and reached $R^2 = 0.8959$ and $R^2 = 0.8932$, respectively. It was found that organic matter transfer to the dissolved phase was affected to a greater extent by the heating method than by the heating temperatures in the analyzed range (Figure 1).

The results of a study conducted by Abdelhay et al. (2020) [34] also proved UD to be an effective technique for post-slaughter wastewater pre-treatment. High-frequency UD may aid conventional treatment methods by promoting the initial oxidation of resistant organic pollutants. The study tested the influence of frequencies reaching 578, 800, and 1142 kHz, and a power density ranging from 160 W/dm³ to 1200 W/dm³. At low power densities, the high frequency (1142 kHz) was more efficient in COD removal than the low one. In contrast, the low-frequency sonication (578 kHz) resulted in a higher COD load removed at high power densities. The highest COD removal percentage, i.e., 49%, and thus the highest increase in COD concentration in the dissolved phase, was achieved at the frequency of

578 kHz and a power density of 480 W/dm³ [34]. In turn, Erden et al. (2010) [35] used a low-frequency UD, i.e., 20 kHz, as a stage of pre-treatment of wastewater from the meat processing industry. The specific energy input ranged from 0 to 50 MJ/kgTS. The study proved the low-frequency UD to be highly effective in increasing the extent of dissolution of organic compounds. The concentration of TOC in the dissolved phase of non-pre-treated wastewater was 557 mg/dm³. The maximal TOC concentration, reaching 654 mg/dm³, was achieved for the UD energy input of 120 MJ/kgTS. Higher UD energies ensured partial mineralization of organic matter preceding the solubilization of the solid phase and TOC concentration decrease in the dissolved phase [35]. In another study, UD with the frequency of 20 kHz and power density of 500 W was used for the pre-treatment of olive mill wastewater (OMW), being one of the most complex types of industrial wastewater. The UD was applied for raw and tenfold-diluted OMW. This study demonstrated a small increase in the COD concentration in the dissolved phase of raw OMW (40,510 mg/dm³), reaching ca. 4–5% after 2 minutes of sonication (ca. 42,535 mg/dm³). This value remained unchanged in the sonicated sample within 10 min since UD. In the case of the diluted OMW, after 10 minutes of sonication, the concentration of soluble COD increased by ca. 23% compared to the raw OMW, approximating 49,827 mg/dm³. In addition, the cited study analyzed the effect of UD lasting 0 to 60 min; however, it failed to demonstrate any successive increase in the COD concentration in the dissolved phase after 10 minutes of sonication [35].

3.2. Anaerobic Digestion

In S0, the biogas yield ranged from 381 ± 33 cm³/gCOD (V3) to 423 ± 27 cm³/gCOD (V1) (Figure 2a), whereas the CH₄ content of the biogas ranged from 60.2 ± 5.1% to 64.0 ± 3.9 (Table 4). The observed differences were not statistically significant (Figure 2b). The initial OLR applied affected the kinetics of methane fermentation, with the *r* value reaching 7.1 ± 0.4 cm³/gCOD·h in V1, 6.0 ± 0.2 cm³/gCOD·h in V2, and 3.2 ± 0.3 cm³/gCOD·h in V3 (Table 4).

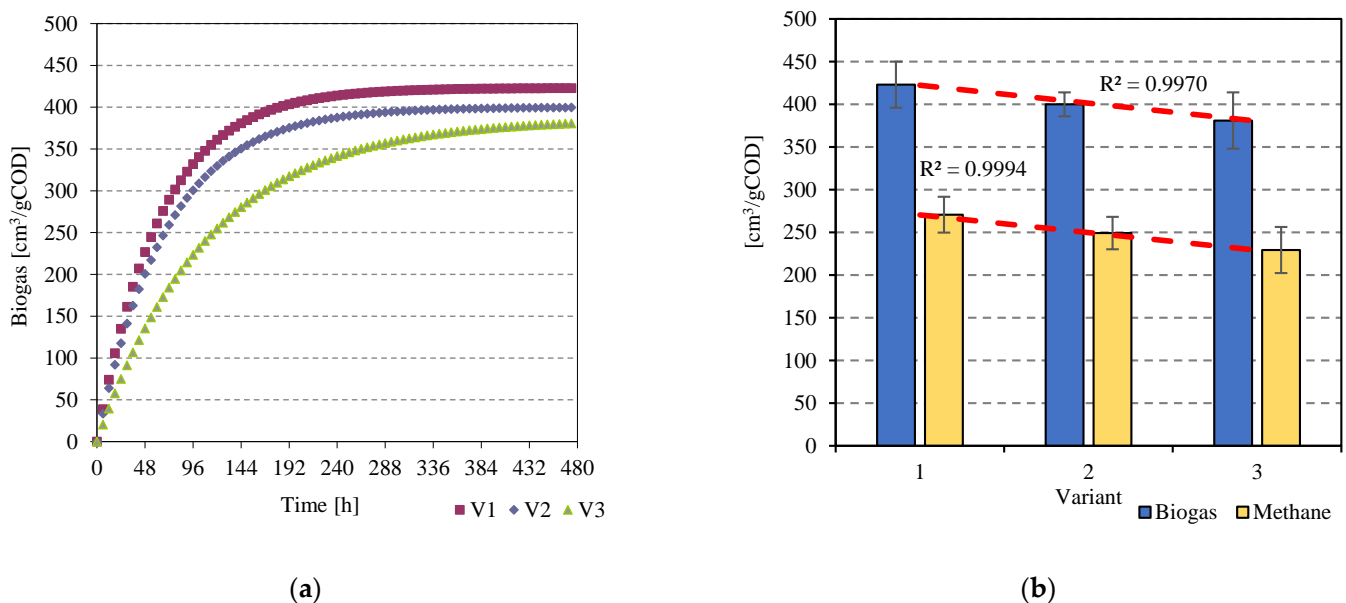


Figure 2. The course of AD process (a) and correlations between OLRs applied and biogas and methane yields (b) achieved in S0.

Table 4. Characteristics of the kinetics of AD process in individual experimental variants.

Indicator	Parameter	Unit	Stage/Variant		
			Stage 0		
			Variant 1	Variant 2	Variant 3
Biogas	Rate (r)	cm ³ /gCOD·h	7.1 ± 0.4	6.0 ± 0.2	3.2 ± 0.3
	Production rate constant (k)	[1/h]	0.10 ± 0.01	0.09 ± 0.01	0.05 ± 0.01
Methane	Methane content	%	64.0 ± 3.9	62.3 ± 2.1	60.2 ± 5.1
	Rate, r	cm ³ /gCOD· h	0.10 ± 0.01	0.08 ± 0.01	0.05 ± 0.01
	Production rate constant (k)	[1/h]	4.5 ± 0.3	3.3 ± 0.2	1.9 ± 0.2
Indicator	Parameter	Unit	Stage 1		
			Variant 1	Variant 2	Variant 3
			Biogas	Rate, r	cm ³ /gCOD· h
Production rate constant (k)	[1/h]	0.10 ± 0.01		0.09 ± 0.01	0.07 ± 0.01
Methane	Methane content	%	70.4 ± 2.7	69.2 ± 4.3	67.9 ± 3.1
	Rate, r	cm ³ /gCOD· h	0.10 ± 0.01	0.09 ± 0.01	0.06 ± 0.01
	Production rate constant (k)	[1/h]	5.1 ± 0.2	4.4 ± 0.4	2.6 ± 0.1
Indicator	Parameter	Unit	Stage 2		
			Variant 1	Variant 2	Variant 3
			Biogas	Rate, r	cm ³ /gCOD· h
Production rate constant (k)	[1/h]	0.11 ± 0.01		0.10 ± 0.01	0.09 ± 0.01
Methane	Methane content	%	69.1 ± 2.4	69.0 ± 4.0	67.2 ± 3.1
	Rate, r	cm ³ /gCOD· h	5.1 ± 0.2	4.5 ± 0.3	3.6 ± 0.2
	Production rate constant (k)	[1/h]	0.10 ± 0.01	0.09 ± 0.01	0.08 ± 0.01
Indicator	Parameter	Unit	Stage 3		
			Variant 1	Variant 2	Variant 3
			Biogas	Rate, r	cm ³ /gCOD· h
Production rate constant (k)	[1/h]	0.11 ± 0.01		0.10 ± 0.01	0.10 ± 0.01
Methane	Methane content	%	69.3 ± 1.7	69.9 ± 3.1	68.7 ± 2.2
	Rate, r	cm ³ /gCOD· h	5.5 ± 0.1	4.6 ± 0.2	4.3 ± 0.1
	Production rate constant (k)	[1/h]	0.10 ± 0.01	0.09 ± 0.01	0.09 ± 0.01
Indicator	Parameter	Unit	Stage 4		
			Variant 1	Variant 2	Variant 3
			Biogas	Rate, r	cm ³ /gCOD· h
Production rate constant (k)	[1/h]	0.11 ± 0.01		0.10 ± 0.01	0.09 ± 0.01
Methane	Methane content	%	69.8 ± 1.4	70.6 ± 2.1	70.1 ± 1.7
	Rate, r	cm ³ /gCOD· h	5.7 ± 0.1	4.9 ± 0.2	4.5 ± 0.1
	Production rate constant (k)	[1/h]	0.10 ± 0.01	0.09 ± 0.01	0.09 ± 0.01

The use of CTP in S1 caused a significant increase in the CH₄ concentration in the biogas, which ranged from 67.9 ± 3.1% (V3) to 70.4 ± 2.7% (V1). The volume of biogas produced and the reaction kinetics were statistically comparable to those noted in S0 (Figure 3a). In turn, the study proved the effect of the initial OLR on the final outcomes of anaerobic digestion. The biogas yield reached 432 ± 17 cm³/gCOD in V1 and 390 ± 11 cm³/gCOD in V3 (Figure 3b). Similar, statistically comparable results were achieved in S2 (Figure 4a). In this stage of the experiment, the biogas yield ranged from 406 ± 11 cm³/gCOD (V3) to 443 ± 16 cm³/gCOD (V1) and was found to depend on the initial OLR (Figure 4b). The CH₄ content of the biogas fell within a narrow range from 67.2 ± 3.1% to 69.1 ± 2.4%, which allowed the yield to range from 272 ± 13 cm³/gCOD to 306 ± 12 cm³/gCOD (Table 4, Figure 4a). The differences observed between variants V1 and V3 were statistically significant. The values describing anaerobic digestion kinetics were comparable to those obtained in S1 (Table 4). The present study proved a significant effect of CTP on the increased CH₄ w content in the biogas and on the total produced volume of this biogas fraction (Table 4). Differences were observed between S0, S1, and S2. In the case of biogas yield, significantly higher values were determined in S2 than in S0. The final values of AD efficiency indicators were similar regardless of the CTP temperature applied in S1 and S2.

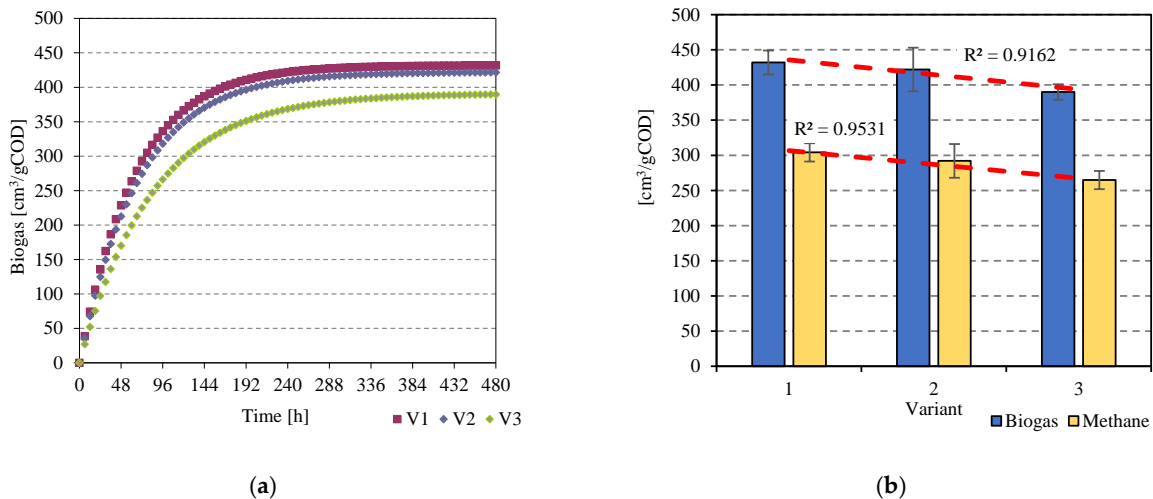


Figure 3. The course of AD process (a) and correlations between OLRs applied and biogas and methane yields (b) achieved in S1.

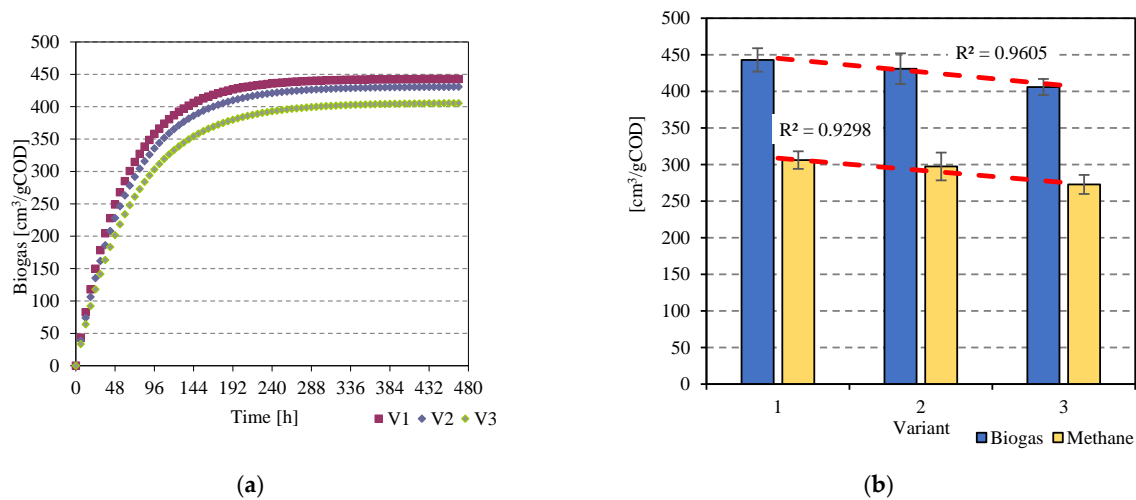


Figure 4. The course of the AD process (a) and correlations between OLRs applied and biogas and methane yields (b) achieved in S2.

Higher AD efficiency was noted upon the use of UTP; however, the differences observed were significantly affected by the heating method and not by the heating temperature. This means that greater differences of the monitored indicators were revealed between S1 (CTP, 70 °C) and S3 (UTP, 70 °C) as well as between S2 (CTP, 90 °C) and S4 (UTP, 90 °C). In S3, the biogas yield ranged from $415 \pm 19 \text{ cm}^3/\text{gCOD}$ to $480 \pm 11 \text{ cm}^3/\text{gCOD}$ and was observed to decrease significantly along with an increasing initial OLR (Figure 5a,b). The CH_4 content of biogas was similar in all variants and ranged from $68.7 \pm 2.2\%$ (V3) to $69.9 \pm 3.1\%$ (V2). The rate of biogas production (r) ranged from $6.9 \pm 0.3 \text{ cm}^3/\text{gCOD} \cdot \text{h}$ to $8.8 \pm 0.2 \text{ cm}^3/\text{gCOD} \cdot \text{h}$, whereas k constant values ranged from 0.10 ± 0.01 to 0.11 ± 0.01 (Table 4). The highest AD efficiency was determined in S4V1 (Figure 6a). The biogas production rate and biogas yield achieved in this variant reached $9.0 \pm 0.2 \text{ cm}^3/\text{gCOD} \cdot \text{h}$ and $492 \pm 10 \text{ cm}^3/\text{gCOD}$, respectively (Figure 6b). Biogas produced contained $69.8 \pm 1.4\% \text{ CH}_4$, enabling a biogas yield at $343 \pm 7 \text{ cm}^3\text{CH}_4/\text{gCOD}$, which approximated the maximal theoretical CH_4 production from 1.0 g COD ($350 \text{ cm}^3\text{CH}_4/\text{gCOD}$). The CH_4 yields noted in V2 and V3 were significantly lower and reached $325 \pm 11 \text{ cm}^3\text{CH}_4/\text{gCOD}$ ($70.6 \pm 2.1\%$) and $302 \pm 8 \text{ cm}^3\text{CH}_4/\text{gCOD}$ ($70.1 \pm 1.7\%$), respectively. The highest CH_4 production rate, i.e., $5.7 \text{ cm}^3/\text{gCOD} \cdot \text{h}$, was determined in V1. The rates noted in V2 and V3 were significantly lower and reached $4.9 \pm 0.2 \text{ cm}^3/\text{gCOD} \cdot \text{h}$ and $4.5 \pm 0.1 \text{ cm}^3/\text{gCOD} \cdot \text{h}$, respectively (Table 4).

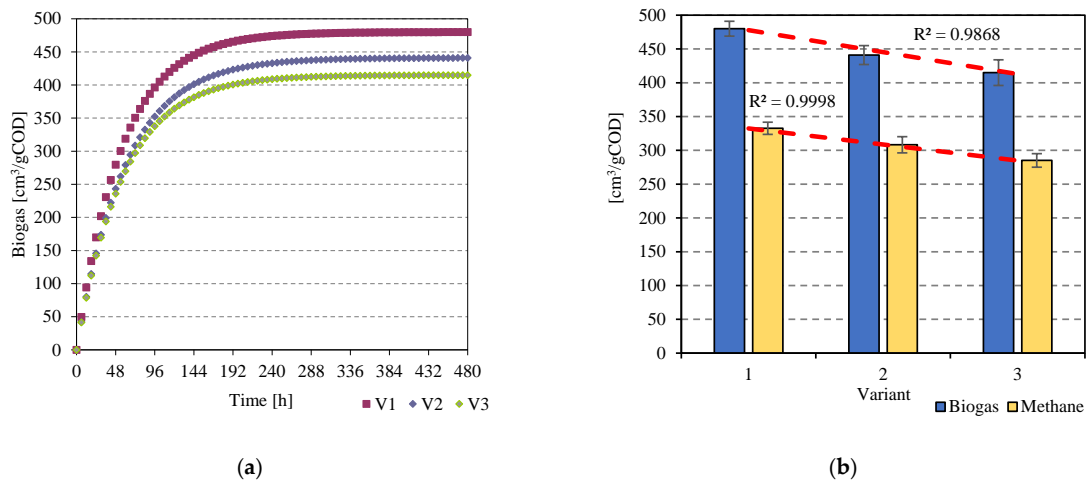


Figure 5. The course of the AD process (a) and correlations between OLRs applied and biogas and methane yields (b) achieved in S3.

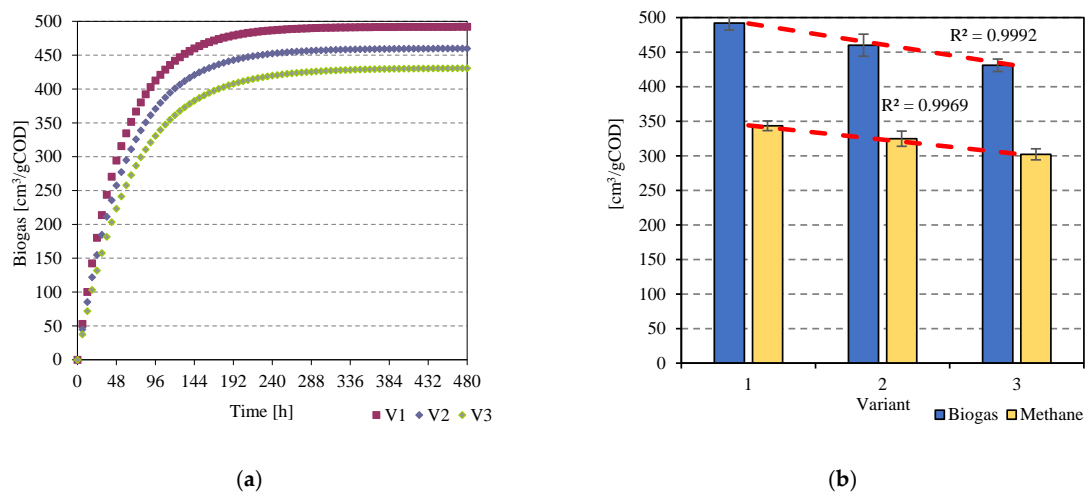


Figure 6. The course of the AD process (a) and correlations between OLRs applied and biogas and methane yields (b) achieved in S4.

The study conducted by Erden et al. (2010) [35] aimed to evaluate the effect of low-frequency ultrasound pre-treatment (20 kHz) on the anaerobic biodegradation of meat processing effluent. Experiments were performed for 50 days for the effluents treated at three specific energy inputs, i.e., 2, 120, and 750 MJ/kgTS, and for the non-pre-treated effluent. Methane production ceased almost completely after 30 days in all variants. The highest methane yield, i.e., 376 cm³, was determined in the variant with the specific energy input of 120 MJ/kg. In the case of the non-pre-treated effluent, the methane yield was barely 304 cm³, indicating that the use of ultrasounds may ensure a 24% increase in methane production. The highest energy input tested, i.e., 750 MJ/kgTS, ensured a ca. 18.5% increase in the methane production yield, due to the diminished availability of organic matter in the dissolved phase [35]. Another study evaluated the effect of UD exposure time from 300 to 1200 s on the anaerobic digestion of dairy wastewater [36]. The volume of methane produced was observed to increase along with a UD extension from 300 to 900 s. The highest methane yield, i.e., 0.203 ± 0.01 dm³CH₄/gCOD, was achieved during 900-s sonication, after which the methane content of the biogas reached 70.9 ± 2.8%. Extending disintegration to 1200 s had no significant effect on the methane fermentation efficiency [36]. In turn, Nour (2015) [37] used the ultrasonic membrane anaerobic system (UMAS) for the treatment of undiluted slaughterhouse wastewater. The frequency of ultrasounds was 25 KHz. Biogas production increased along with an increasing OLR, from 0.29 dm³/gCOD·d at OLR = 0.5 kgCOD/m³·d to 0.88 dm³/gCOD·d at OLR = 9.5 kg kgCOD/m³·d. In contrast, the content of methane in the biogas was observed to decrease along with an increasing OLR and fitted within the range from 68.5% to 79%. The methane content decrease was ascribed to a higher OLR promoting the growth of acidogenic bacteria instead of the methanogenic ones [37].

3.3. Energy Balance

The thermal pre-treatment of the H-LSPW was conducted in the IS-1K reactor with an active volume of 1.0 dm³. Depending on the experimental variant, the assumed heating temperature was achieved by means of electrical heaters (CTP) or ultrasounds (UTP). It needs to be emphasized that H-LSPW was category 3 waste, which requires pre-disintegration to the maximal particle diameter of 60 mm and then 60-minute retention at a temperature of 70 °C prior to the AD process, as stipulated in the legal regulations in force [38]. Hence, the thermal pre-treatment is an indispensable technological procedure that cannot be eliminated [39]. Given the above, there emerges a justified need to search for a method of heat energy supply, in the case of which the process of anaerobic disintegration of this type of waste would be technologically, energetically, and environmentally viable.

The energy balance performed proved substrate heating to 70 °C to be the most advisable variant of thermal pre-treatment, regardless of whether the heating proceeded via CTP or UTP (Table 5). Considering the volume of biogas produced, methane content, and unit energy value of this biogas fraction, reaching 0.00917 Wh/dm³, the highest gross energetic efficiency was demonstrated in variants S4V3 (UTP 90 °C, OLR = 6.0 gCOD/dm³) and S3V3 (UTP 70 °C, OLR = 6.0 gCOD/dm³), i.e., 11.84 ± 0.24 Wh and 11.41 ± 0.27 Wh, respectively. In S0V3 (control, OLR = 6.0 gCOD/dm³), without the pre-treatment, the energy content of the produced CH₄ was significantly lower and reached 10.48 ± 0.74 Wh (Table 5). Taking into account the energy inputs, the highest net energy efficiencies were determined in S1V3 (CTP 70 °C, OLR = 6.0 gCOD/dm³) and S3V3 (UTP 70 °C, OLR = 6.0 gCOD/dm³), and reached 5.92 ± 0.43 Wh and 5.80 ± 0.42, respectively (Table 5). The observed differences were not statistically significant. The net energy gain achieved in the remaining thermal pre-treatment variants was significantly lower, ranging from 2.00 ± 0.13 Wh (S2V1) to 4.98 ± 0.42 Wh (S2V3). The energetic efficiency obtained was found to be influenced to the greatest extent by the OLRs applied. This was mainly reflected in the lowest total CH₄ yield noted at OLR = 6.0 gCOD/dm³ (V3). Due to the active volume of respirometers (500 cm³), the OLR was 3.0 gCOD in these variants. Depending on the experimental stage, this variant yielded from 795 ± 48 cm³CH₄ (S1V3) to 906 ± 24 cm³CH₄ (S4V3). In the variants with

the initial OLR = 2.0 gCOD/dm³, the total volume of CH₄ produced was lower (Table 5) and ranged from 304 ± 13 cm³CH₄ (S1V1) to 343 ± 7 cm³CH₄ (S4V1). Despite the control stage (S0) producing the lowest total CH₄ yields, ranging from 270 ± 21 cm³CH₄ (S0V1) to 687 ± 81 cm³CH₄ (SE0V3), it yielded the highest net energy, i.e., 10.48 ± 0.74 (S0V3). This was due to the fact that H-LSPW was not pre-treated at this stage, hence the gross energy determined in CH₄ was the same as the net energy. It should be again emphasized that H-LSPW is a category 3-type waste requiring substrate pre-treatment prior to AD and increasing energy expenditure. Other researchers have also demonstrated that UD generates additional energy expenditures for the wastewater treatment system [40]. It was found, however, that an appropriate technology can be coupled with anaerobic digesters to facilitate the stage of hydrolysis and boost the efficiency of complex wastewater treatment systems [41].

Table 5. Energy balance of thermal pre-treatment of H-LSPW in individual experimental variants.

Stage	Variant	E _{sin.} [Wh]	COD _{in} [g]	E _{in} [Wh/gCOD]	M _{CODin} [g]	E _{totinR} [Wh]	CH _{4R} [cm ³ /gCOD]	Y _{CH4out} [cm ³]	E _{CH4} [Wh/cm ³]	E _{CH4out} [Wh]	E _{net} [Wh]
0	1	0	72.9 ± 4.95	0	1	0	270 ± 21	270 ± 21	0.00917	3.88 ± 0.19	3.88 ± 0.19
	2				2		249 ± 19	498 ± 38		7.33 ± 0.35	7.33 ± 0.35
	3				3		229 ± 27	687 ± 81		10.48 ± 0.74	10.48 ± 0.74
Stage	Variant	E _{sin.} [Wh]	COD _{in} [g]	E _{in} [Wh/gCOD]	M _{CODin} [g]	E _{totinR} [Wh]	CH _{4R} [cm ³ /gCOD]	Y _{CH4out} [cm ³]	E _{CH4} [Wh/cm ³]	E _{CH4out} [Wh]	E _{net} [Wh]
1	1	116 ± 9	72.9 ± 4.95	1.60 ± 0.14	1	1.60 ± 0.14	304 ± 13	304 ± 13	0.00917	3.96 ± 0.12	2.36 ± 0.13
	2				2	3.20 ± 0.28	292 ± 24	584 ± 48		7.73 ± 0.44	4.53 ± 0.36
	3				3	4.80 ± 0.42	265 ± 16	795 ± 48		10.72 ± 0.44	5.92 ± 0.43
Stage	Variant	E _{sin.} [Wh]	COD _{in} [g]	E _{in} [Wh/gCOD]	M _{CODin} [g]	E _{totinR} [Wh]	CH _{4R} [cm ³ /gCOD]	Y _{CH4out} [cm ³]	E _{CH4} [Wh/cm ³]	E _{CH4out} [Wh]	E _{net} [Wh]
2	1	150 ± 12	72.9 ± 4.95	2.06 ± 0.16	1	2.06 ± 0.16	306 ± 12	306 ± 12	0.00917	4.06 ± 0.11	2.00 ± 0.13
	2				2	4.12 ± 0.32	297 ± 19	595 ± 38		7.90 ± 0.35	3.78 ± 0.33
	3				3	6.18 ± 0.48	273 ± 13	818 ± 39		11.16 ± 0.36	4.98 ± 0.42
Stage	Variant	E _{sin.} [Wh]	COD _{in} [g]	E _{in} [Wh/gCOD]	M _{CODin} [g]	E _{totinR} [Wh]	CH _{4R} [cm ³ /gCOD]	Y _{CH4out} [cm ³]	E _{CH4} [Wh/cm ³]	E _{CH4out} [Wh]	E _{net} [Wh]
3	1	136 ± 17	72.9 ± 4.95	1.87 ± 0.19	1	1.87 ± 0.19	332 ± 9	332 ± 9	0.00917	4.40 ± 0.08	2.53 ± 0.17
	2				2	3.74 ± 0.38	308 ± 12	616 ± 24		8.08 ± 0.22	4.34 ± 0.30
	3				3	5.61 ± 0.57	285 ± 10	855 ± 30		11.41 ± 0.27	5.80 ± 0.42
Stage	Variant	E _{sin.} [Wh]	COD _{in} [g]	E _{in} [Wh/gCOD]	M _{CODin} [g]	E _{totinR} [Wh]	CH _{4R} [cm ³ /gCOD]	Y _{CH4out} [cm ³]	E _{CH4} [Wh/cm ³]	E _{CH4out} [Wh]	E _{net} [Wh]
4	OLR2	180 ± 19	72.9 ± 4.95	2.46 ± 0.21	1	2.46 ± 0.21	343 ± 7	343 ± 7	0.00917	4.5 ± 0.06	2.04 ± 0.14
	OLR4				2	4.92 ± 0.42	325 ± 11	650 ± 22		8.43 ± 0.20	3.51 ± 0.31
	OLR6				3	7.38 ± 0.63	302 ± 8	906 ± 24		11.84 ± 0.24	4.46 ± 0.42

3.4. Empirical Models

A multiple regression method was harnessed to develop empirical equations enabling the estimation of biogas and methane yields in methane fermentation. It was found that biogas and methane yields were statistically significantly affected by such dependent variables as OLR as well as TOC concentrations in the supernatant. The postulated model of biogas yield (5) is characterized by an estimation error of ± 8.7437 and reflects ca. 91.99% of changes in the process of biogas production ($R^2 = 0.9199$). The methane yield model (6) reflects ca. 91.38% changes in the process of its production ($R^2 = 0.9138$) with an estimation error of ± 13.384 . Figure 7 shows the forecasted impact of the COD concentration in the supernatant and OLR on biogas and methane yields.

$$\text{BIOGAS} = 0.0079\text{TOC} - 12.35\text{OLR} + 365.9324 \quad (5)$$

$$\text{METHANE} = 0.0084\text{TOC} - 10.1389\text{OLR} + 211.9114 \quad (6)$$

BIOGAS—biogas yield, cm^3/gCOD ;

METHANE—methane yield, $\text{cm}^3\text{CH}_4/\text{gCOD}$;

TOC—TOC concentration in the supernatant, mgO_2/dm^3 ; and

OLR—initial organic load rate (OLR) of anaerobic respirometers, gCOD/dm^3

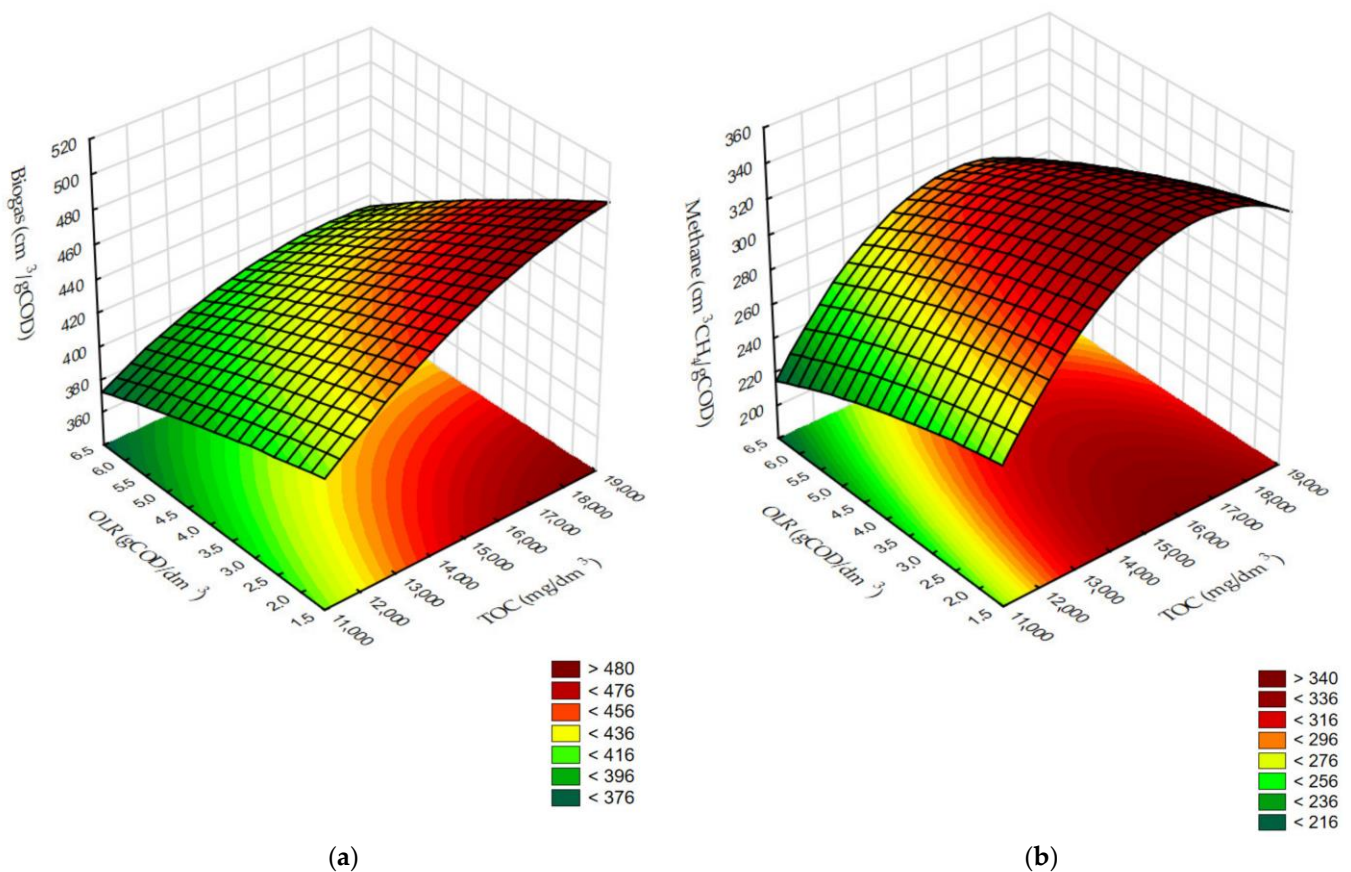


Figure 7. Surface correlation between COD concentration in the supernatant and OLR and the (a) biogas and (b) methane yields.

4. Conclusions

Legal regulations in force in the EU impose an obligation of thermal pre-treatment of post-slaughter waste prior to its methane fermentation. Due to the increasingly fewer use of cogeneration systems in favor of biomethane production to supply gas networks or vehicles of road transport, there is a need to look for alternative heating methods. The

presented research verified the synergistic effect of simultaneous heating and ultrasonic disintegration on the technological effect and energy balance of the anaerobic digestion of highly-loaded slaughter poultry wastewater (H-LSPW).

The analysis of changes in the concentrations of organic compounds in the dissolved phase enables us to conclude that the pre-treatment efficiency was affected by the method of H-LSPW heating and by the heating temperatures tested. The use of the combined process of heating and ultrasonic disintegration (UTP) allowed for a significant increase in the content of organic matter in the dissolved phase compared to conventional heating (CTP).

The highest AD technological effects related to the volume of biogas produced, methane content and process kinetics were obtained for the H-LSPW pre-treated with ultrasounds (UTP). The assessed indicators of methane fermentation were also significantly affected by the initial OLR applied. It was proved that the biogas yield and the methane content per unit mass of COD feedstock decreased along with OLR increase. A higher total production of gaseous metabolites of anaerobic bacteria was obtained as well.

The higher technological effects of AD of wastewater subjected to UTP were not reflected in the net energy production, mainly because UTP is more energy-intensive and, hence, the higher gross energy production in CH₄ was offset by a higher energy consumption in the thermal pre-treatment.

Author Contributions: Conceptualization, J.K. and M.D.; methodology, J.K. and M.D.; validation, J.K.; formal analysis, J.K. and M.D.; investigation, J.K., M.D. and M.Z.; resources, J.K., M.D. and M.Z.; software, J.K.; data curation, J.K., M.D. and M.Z.; supervision, J.K.; project administration, M.Z.; writing—original draft preparation, J.K. and M.D.; writing—review and editing, J.K., M.D. and M.Z.; visualization, J.K. and M.D.; funding acquisition, J.K. All authors have read and agreed to the published version of the manuscript.

Funding: The manuscript was supported by Project financially supported by Minister of Education and Science in the range of the program entitled “Regional Initiative of Excellence” for the years 2019–2022, project no. 010/RID/2018/19, amount of funding: 12,000,000 PLN, and the work WZ/WB-IIS/3/2022, funded by the Minister of Education and Science.

Institutional Review Board Statement: Not applicable.

Informed Consent Statement: Not applicable.

Data Availability Statement: Not applicable.

Conflicts of Interest: The authors declare no conflict of interest.

References

1. Trajer, M.; Mieczkowski, M. Trends in poultry consumption after Poland's accession to the European Union. In Proceedings of the International Scientific Conference “Economic Sciences for Agribusiness and Rural Economy”, Warsaw, Poland, 7–8 June 2018. No. 2. [CrossRef]
2. Poultry World. Demand for Poultry Meat in EU Set to Slow. Available online: <https://www.poultryworld.net/poultry/demand-for-poultry-meat-in-eu-set-to-slow/> (accessed on 9 December 2022).
3. Cybulska, K.; Kołosowska, I.; Kramkowski, K.; Karpińska, M.; Roszkowicz-Ostrowska, K.; Kowalczyk, P. Improvement of Biogas Yield by Pre-Treating Poultry Waste with Bacterial Strains. *Energies* **2021**, *14*, 5601. [CrossRef]
4. Mesinger, D.; Ociczek, A. Risk Assessment of Wild Game Meat Intake in the Context of the Prospective Development of the Venison Market in Poland. *Pol. J. Environ. Stud.* **2021**, *30*, 1307–1315. [CrossRef]
5. Mpofu, A.; Kibangou, V.; Kaira, W.; Oyekola, O.; Welz, P. Anaerobic Co-Digestion of Tannery and Slaughterhouse Wastewater for Solids Reduction and Resource Recovery: Effect of Sulfate Concentration and Inoculum to Substrate Ratio. *Energies* **2021**, *14*, 2491. [CrossRef]
6. Rao, M.; Bast, A.; de Boer, A. Valorized Food Processing By-Products in the EU: Finding the Balance between Safety, Nutrition, and Sustainability. *Sustainability* **2021**, *13*, 4428. [CrossRef]
7. European Parliament and of the Council. Regulation (EC) No 1069/2009 of the European Parliament and of the Council of 21 October 2009 Laying down Health Rules as Regards Animal by-Products and Derived Products Not Intended for Human Consumption and Repealing Regulation (EC) No 1774/2002 (Animal by-products Regulation). *Off. J. Eur. Union* **2009**, *300*, 1–33.
8. Socas-Rodríguez, B.; Álvarez-Rivera, G.; Valdés, A.; Ibáñez, E.; Cifuentes, A. Food by-products and food wastes: Are they safe enough for their valorization? *Trends Food Sci. Technol.* **2021**, *114*, 133–147. [CrossRef]

9. Commission Regulation (EU). Commission Regulation (EU) No 142/2011 of 25 February 2011 Implementing Regulation (EC) No 1069/2009 of the European Parliament and of the Council Laying down Health Rules as Regards Animal by-Products and Derived Products Not Intended for Human Consumption. *Off. J. Eur. Union* **2011**, *54*, 1–254.
10. Scherzinger, M.; Kaltschmitt, M. Thermal pre-treatment options to enhance anaerobic digestibility—A review. *Renew. Sustain. Energy Rev.* **2021**, *137*, 110627. [[CrossRef](#)]
11. Izydorczyk, G.; Mikula, K.; Skrzypczak, D.; Witek-Krowiak, A.; Mironiuk, M.; Furman, K.; Gramza, M.; Moustakas, K.; Chojnacka, K. Valorization of poultry slaughterhouse waste for fertilizer purposes as an alternative for thermal utilization methods. *J. Hazard. Mater.* **2022**, *424*, 127328. [[CrossRef](#)]
12. Asses, N.; Farhat, W.; Hamdi, M.; Bouallagui, H. Large scale composting of poultry slaughterhouse processing waste: Microbial removal and agricultural biofertilizer application. *Process. Saf. Environ. Prot.* **2019**, *124*, 128–136. [[CrossRef](#)]
13. Pandit, S.; Savla, N.; Sonawane, J.M.; Sani, A.M.; Gupta, P.K.; Mathuriya, A.S.; Rai, A.K.; Jadhav, D.A.; Jung, S.P.; Prasad, R. Agricultural Waste and Wastewater as Feedstock for Bioelectricity Generation Using Microbial Fuel Cells: Recent Advances. *Fermentation* **2021**, *7*, 169. [[CrossRef](#)]
14. Dalke, R.; Demro, D.; Khalid, Y.; Wu, H.; Urgun-Demirtas, M. Current status of anaerobic digestion of food waste in the United States. *Renew. Sustain. Energy Rev.* **2021**, *151*, 111554. [[CrossRef](#)]
15. Hiloidhari, M.; Kumari, S. Biogas upgrading and life cycle assessment of different biogas upgrading technologies. In *Emerging Technologies and Biological Systems for Biogas Upgrading*; Academic Press: Cambridge, MA, USA, 2021; pp. 413–445. [[CrossRef](#)]
16. Bedoić, R.; Špehar, A.; Puljko, J.; Čuček, L.; Čosić, B.; Pukšec, T.; Duić, N. Opportunities and challenges: Experimental and kinetic analysis of anaerobic co-digestion of food waste and rendering industry streams for biogas production. *Renew. Sustain. Energy Rev.* **2020**, *130*, 109951. [[CrossRef](#)]
17. Dębowski, M.; Kazimierowicz, J.; Świca, I.; Zieliński, M. Ultrasonic Disintegration to Improve Anaerobic Digestion of Microalgae with Hard Cell Walls—*Scenedesmus* sp. and *Pinnularia* sp. *Plants* **2023**, *12*, 53. [[CrossRef](#)]
18. Ali, M.M.; Mustafa, A.M.; Zhang, X.; Zhang, X.; Danhassaan, U.A.; Lin, H.; Choe, U.; Wang, K.; Sheng, K. Combination of ultrasonic and acidic pretreatments for enhancing biohythane production from tofu processing residue via one-stage anaerobic digestion. *Bioresour. Technol.* **2022**, *344*, 126244. [[CrossRef](#)] [[PubMed](#)]
19. Dai, J.; Bai, M.; Li, C.; Cui, H.; Lin, L. Advances in the mechanism of different antibacterial strategies based on ultrasound technique for controlling bacterial contamination in food industry. *Trends Food Sci. Technol.* **2020**, *105*, 211–222. [[CrossRef](#)]
20. Rahman, M.; Lamsal, B.P. Ultrasound-assisted extraction and modification of plant-based proteins: Impact on physicochemical, functional, and nutritional properties. *Compr. Rev. Food Sci. Food Saf.* **2021**, *20*, 1457–1480. [[CrossRef](#)]
21. Wang, Z.; Fang, R.; Guo, H. Advances in ultrasonic production units for enhanced oil recovery in China. *Ultrason. Sonochemistry* **2020**, *60*, 104791. [[CrossRef](#)]
22. Kong, Y.; Peng, Y.; Zhang, Z.; Zhang, M.; Zhou, Y.; Duan, Z. Removal of *Microcystis aeruginosa* by ultrasound: Inactivation mechanism and release of algal organic matter. *Ultrason. Sonochem.* **2019**, *56*, 447–457. [[CrossRef](#)]
23. Komarov, S.; Yamamoto, T.; Fang, Y.; Hariu, D. Combined effect of acoustic cavitation and pulsed discharge plasma on wastewater treatment efficiency in a circulating reactor: A case study of Rhodamine B. *Ultrason. Sonochem.* **2020**, *68*, 105236. [[CrossRef](#)]
24. Khavari, M.; Priyadarshi, A.; Hurrell, A.; Pericleous, K.; Eskin, D.; Tzanakis, I. Characterization of shock waves in power ultrasound. *J. Fluid Mech.* **2021**, *915*, R3. [[CrossRef](#)]
25. Wu, W.; Eskin, D.; Priyadarshi, A.; Subroto, T.; Tzanakis, I.; Zhai, W. New insights into the mechanisms of ultrasonic emulsification in the oil–Water system and the role of gas bubbles. *Ultrason. Sonochem.* **2021**, *73*, 105501. [[CrossRef](#)] [[PubMed](#)]
26. Balasubramani, N.; Venezuela, J.; Yang, N.; Wang, G.; StJohn, D.; Dargusch, M. An overview and critical assessment of the mechanisms of microstructural refinement during ultrasonic solidification of metals. *Ultrason. Sonochem.* **2022**, *89*, 106151. [[CrossRef](#)] [[PubMed](#)]
27. Karthikesh, M.S.; Yang, X. The effect of ultrasound cavitation on endothelial cells. *Exp. Biol. Med.* **2021**, *246*, 758–770. [[CrossRef](#)]
28. Ahn, J.-Y.; Chang, S.-W. Effects of Sludge Concentration and Disintegration/Solubilization Pretreatment Methods on Increasing Anaerobic Biodegradation Efficiency and Biogas Production. *Sustainability* **2021**, *13*, 12887. [[CrossRef](#)]
29. Ouahabi, Y.; Bensadok, K.; Ouahabi, A. Optimization of the Biomethane Production Process by Anaerobic Digestion of Wheat Straw Using Chemical Pretreatments Coupled with Ultrasonic Disintegration. *Sustainability* **2021**, *13*, 7202. [[CrossRef](#)]
30. Fernández-Domínguez, D.; Patureau, D.; Houot, S.; Sertillanges, N.; Zennaro, B.; Jimenez, J. Prediction of organic matter accessibility and complexity in anaerobic digestates. *Waste Manag.* **2021**, *136*, 132–142. [[CrossRef](#)]
31. Kazimierowicz, J.; Bartkowska, I.; Walery, M. Effect of Low-Temperature Conditioning of Excess Dairy Sewage Sludge with the Use of Solidified Carbon Dioxide on the Efficiency of Methane Fermentation. *Energies* **2020**, *14*, 150. [[CrossRef](#)]
32. Spyridonidis, A.; Skamagkis, T.; Lambropoulos, L.; Stamatelatos, K. Modeling of anaerobic digestion of slaughterhouse wastes after thermal treatment using ADM. *J. Environ. Manag.* **2018**, *224*, 49–57. [[CrossRef](#)]
33. Preethi; Banu, J.R.; Varjani, S.; Sivashanmugam, P.; Tyagi, V.K.; Gunasekaran, M. Breakthrough in hydrolysis of waste biomass by physico-chemical pretreatment processes for efficient anaerobic digestion. *Chemosphere* **2022**, *294*, 133617. [[CrossRef](#)]
34. Abdelhay, A.; Abu Othman, A.; Albsoul, A. Treatment of slaughterhouse wastewater using high-frequency ultrasound: Optimization of operating conditions by RSM. *Environ. Technol.* **2020**, *42*, 4170–4178. [[CrossRef](#)] [[PubMed](#)]
35. Erden, G.; Buyukkamaci, N.; Filibeli, A. Effect of low frequency ultrasound on anaerobic biodegradability of meat processing effluent. *Desalination* **2010**, *259*, 223–227. [[CrossRef](#)]

36. Kazimierowicz, J.; Zieliński, M.; Bartkowska, I.; Dębowski, M. Effect of Acid Whey Pretreatment Using Ultrasonic Disintegration on the Removal of Organic Compounds and Anaerobic Digestion Efficiency. *Int. J. Environ. Res. Public Health* **2022**, *19*, 11362. [[CrossRef](#)] [[PubMed](#)]
37. Nour, A. The Potentials of Ultrasonic Membrane Anaerobic System (UMAS) in Treating Slaughterhouse Wastewater. In *Research and Practices in Water Quality*; IntechOpen: London, UK, 2014. [[CrossRef](#)]
38. Kazimierowicz, J.; Dzienis, L.; Dębowski, M.; Zieliński, M. Optimisation of methane fermentation as a valorisation method for food waste products. *Biomass Bioenergy* **2021**, *144*, 105913. [[CrossRef](#)]
39. Seruga, P.; Krzywonos, M.; Paluszak, Z.; Urbanowska, A.; Pawlak-Kruczek, H.; Niedźwiecki, Ł.; Pińkowska, H. Pathogen Reduction Potential in Anaerobic Digestion of Organic Fraction of Municipal Solid Waste and Food Waste. *Molecules* **2020**, *25*, 275. [[CrossRef](#)]
40. Apul, O.G.; Sanin, F.D. Ultrasonic pretreatment and subsequent anaerobic digestion under different operational conditions. *Bioresour. Technol.* **2010**, *101*, 8984–8992. [[CrossRef](#)]
41. Oz, N.A.; Uzun, A.C. Ultrasound pretreatment for enhanced biogas production from olive mill wastewater. *Ultrason. Sonochem.* **2015**, *22*, 565–572. [[CrossRef](#)]

Disclaimer/Publisher’s Note: The statements, opinions and data contained in all publications are solely those of the individual author(s) and contributor(s) and not of MDPI and/or the editor(s). MDPI and/or the editor(s) disclaim responsibility for any injury to people or property resulting from any ideas, methods, instructions or products referred to in the content.